energies

MDPI

Article

Multi-Objective Capacity Optimization of Grid-Connected Wind–Pumped Hydro Storage Hybrid Systems Considering Variable-Speed Operation

Yang Li [1,*], Outing Li [1], Feng Wu [1], Shiyi Ma [2], Linjun Shi [1] and Feilong Hong [1]

[1] College of Energy and Electrical Engineering, Hohai University, Nanjing 211100, China; 211606010133@hhu.edu.cn (O.L.); wufeng@hhu.edu.cn (F.W.); 19990041@hhu.edu.cn (L.S.); 221606030017@hhu.edu.cn (F.H.)

[2] China Renewable Energy Engineering Institute, Beijing 100120, China; 13810639756@139.com

* Correspondence: eeliyang@hhu.edu.cn

Abstract: The coordination of pumped storage and renewable energy is regarded as a promising avenue for renewable energy accommodation. Considering wind power output uncertainties, a collaborative capacity optimization method for wind–pumped hydro storage hybrid systems is proposed in this work. Firstly, considering the fluctuation of wind power generation caused by the natural seasonal weather and inherent uncertainties of wind power outputs, a combined method based on the generative adversarial network and K-means clustering algorithm is presented to construct wind power output scenarios. Then, a multi-objective wind–pumped storage system capacity optimization model is established with three objectives consisting of minimizing the levelized cost of energy, minimizing the net load peak–valley difference of regional power grids, and minimizing the power output deviation of hybrid systems. An inner and outer nested algorithm is proposed to obtain the Pareto frontiers based on the strength of the Pareto evolutionary algorithm II. Finally, the complementarity of wind power and pumped storage is illustrated through an analysis of numerical examples, and the advantages of variable-speed pumped storage in complementary operation with wind power over fixed-speed units are verified.

Keywords: wind–pumped hydro storage hybrid systems; capacity configuration; variable-speed pumped storage; multi-objective optimization; scenario generation

Citation: Li, Y.; Li, O.; Wu, F.; Ma, S.; Shi, L.; Hong, F. Multi-Objective Capacity Optimization of Grid-Connected Wind–Pumped Hydro Storage Hybrid Systems Considering Variable-Speed Operation. *Energies* **2023**, *16*, 8113. https://doi.org/10.3390/en16248113

Academic Editor: Mahmoud Bourouis

Received: 16 November 2023
Revised: 14 December 2023
Accepted: 15 December 2023
Published: 17 December 2023

1. Introduction

To achieve the goals of carbon peak and carbon neutralization instituted by the Chinese government, renewable energy (RE) sources like solar photovoltaic (PV), wind, hydropower, geothermal, biomass, tidal, biofuels, and waves are considered to be the future for power systems [1–3]. Of all available RE sources, solar and wind are considered the most abundant, developed, economically viable, and commercially accepted. Large-scale new energy integration also poses great challenges to the stable operation of the power grid due to its natural uncertainty and fluctuation [3–6]. To increase grid stability and overcome the adverse effects of fluctuating power output from RE sources, energy storage is been considered a viable option and is widely employed, especially for off-grid/remote area power supply. As the most economical and mature large-scale energy storage option at present, pumped storage has the advantages of flexible regulation, environmental friendliness, technological maturity, and a large regulation capacity [7,8]. The coordinated development of pumped storage with new energy sources such as wind power could help achieve the friendly grid-connected utilization of new energy, which has attracted widespread attention in recent years.

The coordinated capacity optimization of wind power with pumped storage systems is key to realizing the complementary development of renewable energy and pumped

storage. Many studies selected pumped storage hydro as the energy storage to increase the penetration of new energy. Canales et al. [9] optimized the optimal sizing of renewable energy sources coupled with pumped storage in a standalone hybrid power system. Pradhan et al. [10] proposed a novel solution to handle uncertainties of wind and photovoltaic power in a small island using a seawater pumped storage system. Pali et al. [11] presented an off-grid sustainable power-generation system suitable for the rural areas of developing countries that can meet the daily requirements of local families. Perez-Diaz et al. [12] used an isolated power system as a case study, demonstrating that the consideration of constant start-up costs and ramps of the thermal generating units can yield unrealistic results and that the pumped storage hydropower plant may help reduce system scheduling costs. Bhayo et al. [13] investigated the optimal power management of a pumped hydro storage system for supplying standalone power loads. Zohbi et al. [14] analyzed the design of a pumping station and the performance of a hybrid wind–hydropower plant at two dams in Lebanon to choose the most suitable dam to store the energy surplus produced by wind power at night and handle the significant disharmony between wind energy production and electricity demand. Yao et al. [15] proposed an optimal sizing method for a seawater pumped storage plant with variable-speed units in connected mode on an islanded microgrid to improve the output characteristics of offshore wind power and enhance wind power accommodation. Ma et al. [16] optimized the system design of a proposed hybrid solar–wind–pumped storage system in standalone mode for an isolated microgrid in which the loss of power supply probability was further examined. Gao et al. [17] presented the objectives of minimizing the output fluctuation and variation of load, as well as the output differences in the optimization model of a photovoltaic–wind–pumped storage system. Segurado et al. [18] proposed a methodology to optimize the size and operational strategy of wind-powered desalination and pumped hydro storage systems to minimize the total annualized production costs, maximize the percentage of renewable energy sources in the total power production, and minimize the curtailed wind power. Xu et al. [19] proposed a photovoltaic–wind–hydropower station with a pumped storage installation hybrid energy system, aiming to find the optimal configuration with the maximum power supply reliability and minimum investment. However, the above studies focused on the optimal capacity of hybrid systems in off-grid remote areas or isolated islands, with the objectives of reducing loss of load and renewable energy curtailment.

Wind power has been rapidly developed in recently recent years. To mitigate the negative impacts of integrating wind power into power systems directly, some scholars propose to establish a hybrid energy system including wind power and pumped storage stations to achieve complementary operation from the generation side. In this case, the power output of the integrated wind–pumped storage system will be stable and friendly for the power grid. So, for the grid-connected wind–pumped storage system, the impacts of its operation on the power system should be considered. Yuan et al. [20] proposed a schedule optimization model of a grid-connected wind–pumped storage system considering the peak-shaving demand of the receiving-end power grid. Su et al. [21] proposed a coordination scheme for the grid-connected wind–pumped storage system participating in the electricity market. Wang et al. [22] established an operation optimization model for a wind–PV–pumped storage hybrid system considering multiple objectives of carbon emission reduction and power delivery stability. However, until now, related research on the optimal sizing of grid-connected wind–pumped storage has been rarely investigated. The impacts of the fluctuation and uncertainties of wind power on the techno-economics of the hybrid system should be considered [23,24].

In addition, variable-speed pumped storage units have developed rapidly in recent years [25–27]. Compared with fixed-speed pumped storage units, variable-speed pumped storage units have adjustable pumping power, faster response speed, and a better ability to regulate and control the uncertainty of renewable energy outputs. However, in existing research on the collaborative development of pumped storage and renewable energy

systems, the cooperative configuration of pumped storage with variable-speed units and renewable energy is seldom considered.

Therefore, considering the uncertainty of wind power output, a capacity optimal allocation method for grid-connected wind–pumped hydro storage hybrid systems is proposed in this paper. First, considering the seasonal fluctuation and inherent uncertainty of wind power, a generative adversarial network (GAN) and the K-means clustering algorithm are used to generate multiple typical scenarios. Then, we construct a multi-objective capacity optimization model for wind power–pumped hybrid systems with the objectives of minimizing the levelized cost of energy, peak–valley difference of the net load, and power output deviations of the hybrid system. Also, an efficient algorithm using iterations between the inner and outer optimization problem is developed to solve the proposed model, and a Pareto solution set of the optimal capacity of wind power is obtained. Finally, through the analysis and comparison of numerical examples, the advantages of combining wind power and pumped storage are illustrated, along with the advantages of variable-speed pumped storage and wind power over fixed-speed pumped storage units.

The remainder of this paper is structured as follows. The coordination scheme of the hybrid system is described in Section 2. The scenario of the generation of wind power is described in Section 3. The optimization model is presented in Section 4, including the objectives, constraints, and solving algorithm. The results and discussions are presented in Section 5. Finally, the conclusions are illustrated in Section 6.

2. Coordination Scheme of Wind Power and Pumped Storage

Wind–pumped hydro storage hybrid (WPHSH) systems consist of wind turbines, the upper and lower reservoirs of the pumped hydro storage power station, and a reversible pumped storage pump–turbine unit, as shown in Figure 1. In this configuration, the wind power outputs usually have anti-peak regulation characteristics, increasing the deep peak regulation pressure of the receiving-end power grid. Meanwhile, wind power outputs depend on weather conditions like wind speed, making output difficult to predict accurately. Therefore, the anti-peak regulation characteristics and uncertainty of wind power generation introduce challenges to the safe and stable operation of power grids.

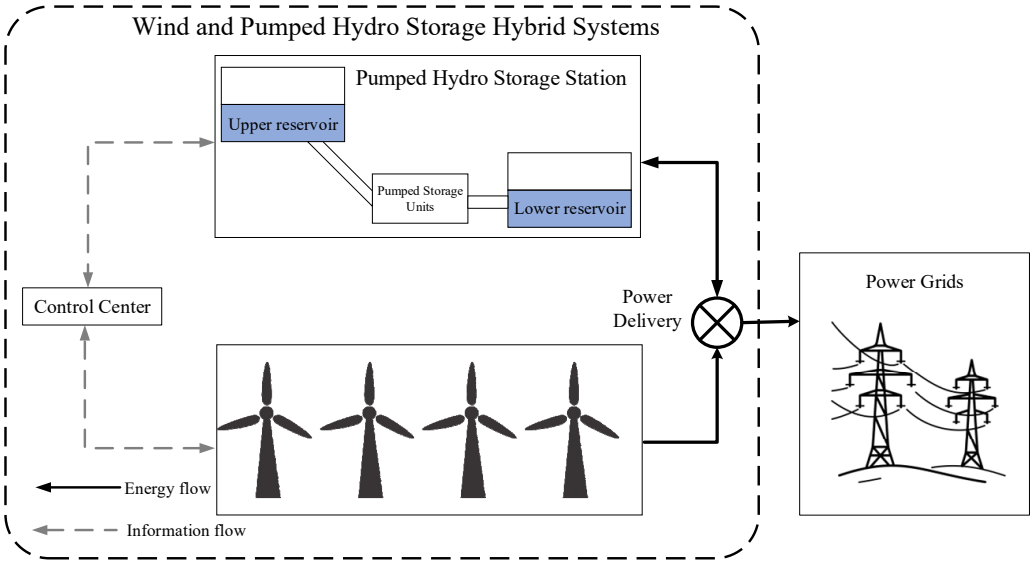

Figure 1. Scheme of wind–pumped hydro storage hybrid systems.

Pumped storage hydropower (PSH) has the advantage of providing fast regulating power for intermittent renewable energy and robustness against weather fluctuation. In this paper, wind power and pumped storage are combined as a hybrid energy system. When

wind power outputs are large and power loads are relatively low, pumped storage can consume wind power, pumping water into the upper reservoir to store energy. Then, during peak load periods, pumped storage generates by releasing water into the lower reservoir. In this case, the anti-peak regulation characteristics can be alleviated. On the other hand, uncertainties of wind power outputs will cause severe power output deviation between the scheduled and actual power delivery, which challenges the stable and economic operation of the power system. In the proposed WPHSH system, the uncertainties of wind power outputs will be compensated for by a pumped storage station to increase the power delivery stability. Therefore, through the coordination of PSH and wind power, the power outputs of the WPHSH system and the loads of power grids can be matched, thus promoting the accommodation of renewable energy generation.

However, for traditional fixed-speed pumped storage units, the pumping power under pumping conditions is fixed. Thus, the regulation capacity of pumped storage units in pumping conditions is limited. With an increase in the penetration of wind power, the regulating ability of PSH in hybrid systems is important. In this case, variable-speed pumped storage units can adjust the pumping power continuously in a certain range by adjusting the speed, which can better adapt to the uncertainty of wind power outputs.

3. Scenario Generation for the Fluctuation and Uncertainty of Wind Power

Due to the fluctuation over a long-time scale (such as one year) and uncertainty over a short time scale (such as one day), the capacity configuration optimization needs to be adapted to the wind power output of all scenarios. In this paper, the seasonal fluctuation of wind power generation in one year and the uncertainty in one day are both simulated using multiple scenarios. Specifically, the power outputs of wind power in one year are represented using the scenarios of typical days. Then, considering the scenarios of typical days, related multiple intra-day scenarios are generated to simulate the uncertainty of wind power, as shown in Figure 2.

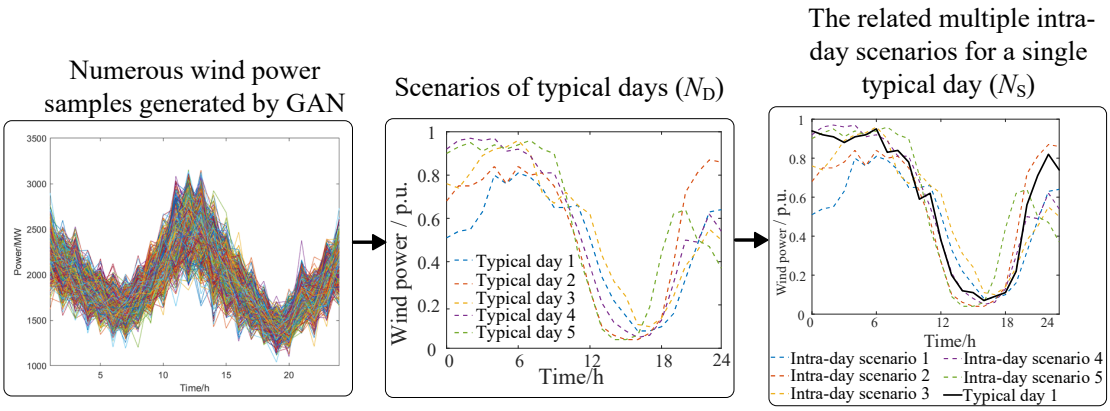

Figure 2. Scheme of the generation of wind power.

Firstly, numerous scenarios of wind power outputs should be acquired. Traditionally, a large number of scenarios are generated using the probability density function of wind power. However, the probability distribution cannot be directly acquired, and it remains difficult to fit the parameters of the probability function when the historical data scale is small. In recent years, artificial intelligence methods have been widely investigated and applied to forecast renewable energy generation. Therefore, the GAN is used to generate numerous scenarios of wind power outputs. A GAN is one of the most powerful generative models and consists of a generator and discriminator.

As shown in Figure 3, the generator attempts to produce samples close to the real data with the given variable vector z, while the target of the discriminator is used to distinguish between samples from actual historical data and generated samples. The generator and

discriminator will make concurrent progress through their continuous interaction in the training process.

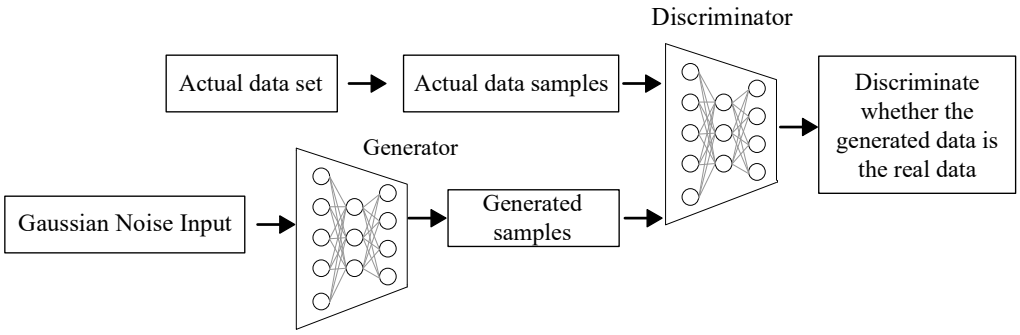

Figure 3. Generation model based on GAN.

For simplicity, we assume that the real historical data of wind power in the WPHSH system are x, and their probability distribution is P_d. There is a set of random noise vectors z whose probability distribution satisfies P_z. A GAN can establish a mapping relationship between P_d and P_z, and the generated samples that satisfy the distribution relationship of the real data by training the generator and discriminator are obtained with probability distribution P_g. The training process is completed via two deep neural networks, namely, the generator $G(z, \theta_G)$ and discriminator $D(x, \theta_D)$, where θ_G and θ_D are the weights of the corresponding neural networks. Therefore, the loss function of a GAN is as follows [28,29]:

$$L_G = E_{z \sim P_z}[-D(G(z))] \tag{1}$$

$$L_D = E_{z \sim P_z}[D(G(z))] - E_{x \sim P_d}[D(x)] \tag{2}$$

where L_G and L_D represent the loss functions of the generator and discriminator, respectively; $E[\cdot]$ is the expectation function; and $G(\cdot)$ and $D(\cdot)$ are, respectively, the generator function and discriminator function. The objective function of the game process is expressed as follows:

$$\min_G \max_D V(G, D) = E_{x \sim P_d}[D(x)] - E_{z \sim P_z}[D(G(z))] \tag{3}$$

Based on the numerous scenarios of wind power output, the K-means clustering method is applied to realize the aggregation of scenarios [30,31].

The specific steps to realize the aggregation of scenarios based on the GAN and K-means clustering method are as follows:

(1) Input historical data and alternately train GAN networks.
(2) Generate a high number of data to establish a dataset of scenarios for wind power output.
(3) Reduce scenarios based on the K-means clustering algorithm to generate representative scenarios of typical days with the number of N_D.
(4) For the representative scenario of one typical day, we choose the related scenarios based on Euclidean distance. In other words, scenarios that are closer to the representative scenario are chosen to formulate related intra-day scenarios based on the K-means clustering method.
(5) Finally, representative scenarios of typical days and related intra-day scenarios are acquired, and the probability of scenarios can also be obtained.

4. Multi-Objective Capacity Optimization Model

4.1. Multiple Objective Functions

This paper comprehensively considers multiple objectives to optimize the installed capacity of wind power generation to coordinate with pumped storage, as the capacity of a pumped storage station is usually limited and determined by natural conditions. Objectives

of the proposed model include minimizing the levelized cost for the energy of WPSHSs, minimizing the peak–valley difference of the power system net load, and minimizing the power output deviations of WPSHSs.

4.1.1. Objective 1: Minimizing the Levelized Cost of Energy (LCOE)

LCOE is the average power generation cost over the entire life cycle of WPSHSs, which is utilized to measure the economy of the project. LCOE is expressed as the ratio of the total cost of WPSHSs to the total power generation, as provided in (4):

$$\min f_{\mathrm{LCOE}} = \frac{C_{\mathrm{inv}} + \sum_{i=1}^{Y_{\mathrm{a}}} \frac{C_{\mathrm{op}} + C_{\mathrm{rp},i}^{\mathrm{w}} + C_{\mathrm{rp},i}^{\mathrm{ps}}}{(1+r)^i} + \sum_{i=1}^{Y_{\mathrm{a}}} \frac{\sum_{k=1}^{N_D} D p_k \sum_{t=1}^{T} a_{\mathrm{s}} \widetilde{P}_{k,t}^{\mathrm{in}}}{(1+r)^i}}{\sum_{i=1}^{Y_{\mathrm{a}}} \frac{D \sum_{k=1}^{N_D} p_k \sum_{t=1}^{T} \widetilde{P}_{k,t}^{\mathrm{out}}}{(1+r)^i}} \tag{4}$$

$$\begin{cases} C_{\mathrm{inv}} = c_{\mathrm{w}} M_{\mathrm{w}} \\ C_{\mathrm{op}} = c_{\mathrm{op}} M_{\mathrm{w}} \end{cases} \tag{5}$$

$$C_{\mathrm{rp},i}^{\mathrm{w}} = \begin{cases} c_{\mathrm{rp,w}}, & \text{if repalced in year } i \\ 0, & \text{if not repalced in year } i \end{cases} \tag{6}$$

$$C_{\mathrm{rp},i}^{\mathrm{ps}} = \begin{cases} c_{\mathrm{rp,ps}}, & \text{if repalced in year } i \\ 0, & \text{if not repalced in year } i \end{cases} \tag{7}$$

where C_{inv} and C_{op} are, respectively, the initial cost of wind power and the annual operational costs of WPHSH systems; $C_{\mathrm{rp},i}^{\mathrm{w}}$ and $C_{\mathrm{rp},i}^{\mathrm{ps}}$ are, respectively, the replacement cost of the wind turbines and the pumped storage units in year i; M_{w} is the total installed capacity of wind turbines; Y_a is the lifetime of hybrid systems, a_{s} is the purchase price of electricity; Y_{w} is the service lifetime of wind turbines; Y_{ps} is the service lifetime of pumped storage units; r is the discount rate; p_k is the probability of the scenario of a typical day k; D is the number of days in a year; $\widetilde{P}_{k,t}^{\mathrm{in}}$ and $\widetilde{P}_{k,t}^{\mathrm{out}}$ are, respectively, the total input and output power of WPHSH systems at time interval t on a typical day k; c_{w} and c_{op} are, respectively, the unit investment and operation costs; $c_{\mathrm{rp,w}}$ and $c_{\mathrm{rp,ps}}$ are, respectively, the replacement cost of wind turbines and pumped storage; N_D is the number of typical daily output scenarios of wind power; and T is a dispatching cycle, which takes 24 h.

4.1.2. Objective 2: Minimizing Peak–Valley Difference (PVD)

In this paper, the peak–valley difference of the power system net load is utilized to reflect the peak-shaving ability of WPSHSs, which is well established in scheduling problems [32–34]. Since wind power generation has large seasonal fluctuations, it is important to optimize the day-ahead schedule of WPHSH systems to minimize the expected peak–valley differences of multiple typical days, expressed as (8)–(11).

$$\min f_{\mathrm{PVD}} = \sum_{k=1}^{N_D} p_k \left(\widetilde{P}_{k,\max}^{\mathrm{net}} - \widetilde{P}_{k,\min}^{\mathrm{net}} \right) \tag{8}$$

$$\widetilde{P}_{k,t}^{\mathrm{net}} = P_{k,t}^{\mathrm{load}} - \widetilde{P}_{k,t}^{\mathrm{out}} + \widetilde{P}_{k,t}^{\mathrm{in}}, \forall k, t \tag{9}$$

$$\widetilde{P}_{k,\max}^{\mathrm{net}} \geq \widetilde{P}_{k,t}^{\mathrm{net}}, \forall k, t \tag{10}$$

$$\widetilde{P}_{k,\min}^{\mathrm{net}} \leq \widetilde{P}_{k,t}^{\mathrm{net}}, \forall k, t \tag{11}$$

where $\widetilde{P}_{k,\max}^{\mathrm{net}}$ and $\widetilde{P}_{k,\min}^{\mathrm{net}}$ are, respectively, the peak and valley values of net load on a typical day k; $P_{k,t}^{\mathrm{load}}$ and $\widetilde{P}_{k,t}^{\mathrm{net}}$ are, respectively, the original and net power loads at time interval t on

a typical day k; and $\widetilde{P}^{\text{out}}_{k,t}$ and $\widetilde{P}^{\text{in}}_{k,t}$ are, respectively, the input and output power of WPSHSs at time interval t on a typical day k.

4.1.3. Objective 3: Minimizing Power Output Deviation (POD)

In (8), for a certain typical day, the scheduled power delivery of the WPHSH operation strategy is optimized. However, the uncertainties of wind power may lead to power deviations in the scheduled and actual power delivery, thereby challenging the stable and economic operation of the power systems. To ensure the reliable operation of the power systems, power output deviation is defined as in (12):

$$\min f_{\text{POD}} = \sum_{k=1}^{N_D} \left\{ p_k \cdot \sum_{s=1}^{N_S} \omega_{k,s} \sum_{t=1}^{T} \left| (\widetilde{P}^{\text{out}}_{k,t} - \widetilde{P}^{\text{in}}_{k,t}) - (P^{\text{out}}_{k,s,t} - P^{\text{in}}_{k,s,t}) \right| \right\} \tag{12}$$

where $P^{\text{in}}_{k,s,t}$ and $P^{\text{out}}_{k,s,t}$ are, respectively, the input and output power of WPHSH systems at time interval t in intra-day scenario s during a typical day k; $\omega_{k,s}$ is the probability of the intra-day scenario s of a typical day k; and N_S is the number of intra-day scenarios of wind power outputs for a single typical day.

4.2. Constraints

4.2.1. Installed Capacity Constraint

The installed capacity of wind power is limited by natural conditions, as shown in (13).

$$0 \le M_{\text{w}} \le M_{\text{w,max}} \tag{13}$$

where $M_{\text{w,max}}$ is the maximum allowable installed capacity of wind turbines.

4.2.2. Operational Constraints

Notably, the scheduling problem of pumped storage and wind power generation is included in the capacity optimization of this system. According to our three objectives (Equations (4), (8), and (12)), both the day-ahead schedule and intra-day operational constraints of WPHSH systems should be considered, as the fluctuation and uncertainty of wind power generation are both complemented by pumped storage.

1. Day-ahead stage operational constraints

The following are the specific hydraulic constraints considered in the day-ahead operation stage.

(1) Reservoir operational constraints

There are two kinds of pumped storage station with and without natural inflows. In this work, a pure pumped storage station storing water in the upper reservoir with no natural water inflows is considered. The water balance and water storage limits are expressed as (14)–(16):

$$\widetilde{V}^{\text{up}}_{k,t} = \widetilde{V}^{\text{up}}_{k,t-1} + \sum_{n=1}^{N_{\text{PS}}} \left(\widetilde{Q}^{\text{p}}_{k,n,t} - \widetilde{Q}^{\text{h}}_{k,n,t} \right) \Delta t, \forall k, t \tag{14}$$

$$V^{\text{up}}_{\min} \le \widetilde{V}^{\text{up}}_{k,t} \le V^{\text{up}}_{\max}, \forall k, t \tag{15}$$

$$\widetilde{V}^{\text{up}}_{k,0} = V^{\text{up}}_{k,\text{begin}}, \widetilde{V}^{\text{up}}_{k,\text{T}} = V^{\text{up}}_{k,\text{end}}, \forall k \tag{16}$$

where $\widetilde{V}^{\text{up}}_{k,t}$ is the water storage of the upper reservoir at time interval t on a typical day k; $\widetilde{Q}^{\text{p}}_{k,n,t}$ and $\widetilde{Q}^{\text{h}}_{k,n,t}$ are, respectively, the pumping and generating water flow of pumped storage unit n at time interval t on a typical day k; $V^{\text{up}}_{\max}$ and $V^{\text{up}}_{\min}$ are, respectively, the maximum and minimum values of the upper reservoir capacity; $V^{\text{up}}_{k,\text{begin}}$ and $V^{\text{up}}_{k,\text{end}}$ are, respectively, the initial water storage and control target of the upper reservoir within a

dispatching horizon on a typical day k; and N_{PS} is the number of units in a pumped storage station.

(2) Power constraints

$$\widetilde{Q}^{\mathrm{h}}_{k,n,t} = \frac{\widetilde{P}^{\mathrm{h}}_{k,n,t}}{\lambda^{\mathrm{h}}_{\mathrm{c}}\lambda_{\mathrm{wp}}\rho g h} = K^{\mathrm{h}}_{\mathrm{c}}\widetilde{P}^{\mathrm{h}}_{k,n,t}, \forall k, n, t \tag{17}$$

$$\widetilde{Q}^{\mathrm{p}}_{k,n,t} = \frac{\lambda^{\mathrm{p}}_{\mathrm{c}}\lambda_{\mathrm{wp}}\widetilde{P}^{\mathrm{p}}_{k,n,t}}{\rho g h} = K^{\mathrm{p}}_{\mathrm{c}}\widetilde{P}^{\mathrm{p}}_{k,n,t}, \forall k, n, t \tag{18}$$

$$U^{\mathrm{h}}_{k,n,t}P^{\mathrm{h}}_{n,\min} \le \widetilde{P}^{\mathrm{h}}_{k,n,t} \le U^{\mathrm{h}}_{k,n,t}P^{\mathrm{h}}_{n,\max}, \forall k, n, t \tag{19}$$

$$U^{\mathrm{p}}_{k,n,t}P^{\mathrm{p}}_{n,\min} \le \widetilde{P}^{\mathrm{p}}_{k,n,t} \le U^{\mathrm{p}}_{k,n,t}P^{\mathrm{p}}_{n,\max}, \forall k, n, t \tag{20}$$

where $\widetilde{P}^{\mathrm{h}}_{k,n,t}$ and $\widetilde{P}^{\mathrm{p}}_{k,n,t}$ are, respectively, the generating and pumping power of pumped storage unit n at time interval t on a typical day k; $\lambda^{\mathrm{h}}_{\mathrm{c}}$ and $\lambda^{\mathrm{p}}_{\mathrm{c}}$ are, respectively, the generating and pumping efficiency of the pumped storage unit; λ_{wp} is the conveying efficiency of the pipeline; $K^{\mathrm{h}}_{\mathrm{c}}$ and $K^{\mathrm{p}}_{\mathrm{c}}$ are, respectively, the ratio between power and flow under generating and pumping operation conditions; ρ is the density of water; g is the gravitational acceleration; h is the water head height; $U^{\mathrm{h}}_{k,n,t}$ and $U^{\mathrm{p}}_{k,n,t}$ are, respectively, the binary variables indicating the on/off status of the generating and pumping conditions of pumped storage unit n at time interval t on a typical day k; $P^{\mathrm{h}}_{n,\max}$ and $P^{\mathrm{h}}_{n,\min}$ are, respectively, the maximum and minimum generating power of pumped storage unit n; and $P^{\mathrm{p}}_{n,\max}$ and $P^{\mathrm{p}}_{n,\min}$ are, respectively, the maximum and minimum pumping power of pumped storage unit n.

The variable speed pumped storage unit can adjust output power under pumping conditions and has stronger adjustment capabilities. For fixed-speed pumped storage units, the power is fixed under pumping conditions, which cannot be adjusted. Thus, the fixed-speed pumped storage units and pumping power constraints (i.e., Equation (20)) are adjusted accordingly:

$$\widetilde{P}^{\mathrm{p}}_{k,n,t} = U^{\mathrm{p}}_{k,n,t}P^{\mathrm{p}}_{n,\max}, \forall k, n, t \tag{21}$$

(3) Unit commitment constraints

Since the pumped storage units in pumped storage power plants share the same waterways under different operating conditions, the same pumped storage unit cannot be in the generating or pumping mode at the same time. This rule also applies to multiple units. The following constraints are designed for the unit states as follows:

$$U^{\mathrm{h}}_{k,n,t} + U^{\mathrm{p}}_{k,n,t} \le 1, \forall k, n, t \tag{22}$$

$$\sum_{n' \ne n}^{N_{\mathrm{PS}}} U^{\mathrm{p}}_{k,n',t} \le (N_{\mathrm{PS}} - 1)(1 - U^{\mathrm{h}}_{k,n,t}), \forall k, t, n \tag{23}$$

(4) Wind power output constraints

$$0 \le \widetilde{P}^{\mathrm{w}}_{k,t} \le M_{\mathrm{w}}\eta^{\mathrm{w}}_{k,t}, \forall k, t \tag{24}$$

$$1 - \frac{\sum_{t=1}^{T}\widetilde{P}^{\mathrm{w}}_{k,t}}{\sum_{t=1}^{T}M_{\mathrm{w}}\eta^{\mathrm{w}}_{k,t}} \le \delta \tag{25}$$

where $\eta^{\mathrm{w}}_{k,t}$ is the coefficient of wind output power; $\widetilde{P}^{\mathrm{w}}_{k,t}$ is the scheduled wind power at time interval t on a typical day k; and δ is the maximum allowed wind power curtailment ratio.

(5) Delivery constraints

$$-P_L \le \widetilde{P}^{\text{out}}_{k,t} - \widetilde{P}^{\text{in}}_{k,t} \le P_L, \forall k, t \tag{26}$$

$$\widetilde{P}^{\text{out}}_{k,t} - \widetilde{P}^{\text{in}}_{k,t} = \widetilde{P}^{\text{w}}_{k,t} + \sum_{n=1}^{N_{\text{PS}}} \left(\widetilde{P}^{\text{h}}_{k,n,t} - \widetilde{P}^{\text{p}}_{k,n,t} \right), \forall k, t \tag{27}$$

where P_L is the maximum transmission capacity of the delivery channel.

2. Intra-day stage operational constraints

Despite day-ahead stage operational constraints, the pumped storage is adjusted in the day-ahead stage to compensate for wind power uncertainty, minimizing the power output deviation of WPHSH systems. In the intra-day stage, the pumped storage is assumed to retain the day-ahead unit commitment schedule to avoid exacerbating the ullage of the units' lives. Therefore, the following constraints, composed of pumped storage unit operation and reservoir operation, are considered:

$$V^{\text{up}}_{k,s,t} = V^{\text{up}}_{k,s,t-1} + \sum_{n=1}^{N_{\text{PS}}} \left(Q^{\text{p}}_{k,s,n,t} - Q^{\text{h}}_{k,s,n,t} \right) \Delta t, \forall k, s, t \tag{28}$$

$$V^{\text{up}}_{\min} \le V^{\text{up}}_{k,s,t} \le V^{\text{up}}_{\max}, \forall k, s, t \tag{29}$$

$$V^{\text{up}}_{k,s,0} = V^{\text{up}}_{k,\text{begin}}, V^{\text{up}}_{k,s,\text{T}} = V^{\text{up}}_{k,\text{end}}, \forall k, s \tag{30}$$

$$Q^{\text{h}}_{k,s,n,t} = \frac{P^{\text{h}}_{k,s,n,t}}{\lambda^{\text{h}}_{\text{c}} \lambda_{\text{wp}} \rho g h} = K^{\text{h}}_{\text{c}} P^{\text{h}}_{k,s,n,t}, \forall k, s, n, t \tag{31}$$

$$Q^{\text{p}}_{k,s,n,t} = \frac{\lambda^{\text{p}}_{\text{c}} \lambda_{\text{wp}} P^{\text{p}}_{k,s,n,t}}{\rho g h} = K^{\text{p}}_{\text{c}} P^{\text{p}}_{k,s,n,t}, \forall k, s, n, t \tag{32}$$

$$U^{\text{h}}_{k,n,t} P^{\text{h}}_{n,\min} \le P^{\text{h}}_{k,s,n,t} \le U^{\text{h}}_{k,n,t} P^{\text{h}}_{n,\max}, \forall k, s, n, t \tag{33}$$

$$U^{\text{p}}_{k,n,t} P^{\text{p}}_{n,\min} \le P^{\text{p}}_{k,s,n,t} \le U^{\text{p}}_{k,n,t} P^{\text{p}}_{n,\max}, \forall k, s, n, t \tag{34}$$

$$0 \le P^{\text{w}}_{k,s,t} \le P^{\text{w}}_{k,s,t,\max}, \forall k, s, t \tag{35}$$

$$-P_L \le P^{\text{out}}_{k,s,t} - P^{\text{in}}_{k,s,t} \le P_L, \forall k, s, t \tag{36}$$

$$P^{\text{out}}_{k,s,t} - P^{\text{in}}_{k,s,t} = P^{\text{w}}_{k,s,t} + \sum_{n=1}^{N_{\text{PS}}} \left(P^{\text{h}}_{k,s,n,t} - P^{\text{p}}_{k,s,n,t} \right), \forall k, s, t \tag{37}$$

where $V^{\text{up}}_{k,s,t}$ is the water storage of the upper reservoir at time interval t in intra-day scenario s of a typical day k; $Q^{\text{p}}_{k,s,n,t}$ and $Q^{\text{h}}_{k,s,n,t}$ are, respectively, the pumping and generating water flow of pumped storage unit n at time interval t in an intra-day scenario s of a typical day k; $P^{\text{h}}_{k,s,n,t}$ and $P^{\text{p}}_{k,s,n,t}$ are, respectively, the generating and pumping power of pumped storage unit n at time interval t in intra-day scenario s of a typical day k; $P^{\text{w}}_{k,s,t}$ and $P^{\text{w}}_{k,s,t,\max}$ are, respectively, the intra-day wind power outputs and maximum wind power outputs at time interval t in intra-day scenario s of a typical day k; and $P^{\text{in}}_{k,s,t}$ and $P^{\text{out}}_{k,s,t}$ are, respectively, the total input and output power of WPHSH systems at time interval t in the intra-day scenario s of a typical day k.

4.3. Optimization Algorithm

The compact form of the proposed capacity model can be expressed as (38):

$$\begin{cases} \min f_{\text{LCOE}}(\boldsymbol{x}, \boldsymbol{y}_1, \boldsymbol{y}_2) \\ \min f_{\text{PVD}}(\boldsymbol{y}_1) \\ \min f_{\text{POD}}(\boldsymbol{y}_1, \boldsymbol{y}_2) \\ s.t.\ g(\boldsymbol{x}) \le 0 \\ \quad h(\boldsymbol{x}, \boldsymbol{y}_1, \boldsymbol{y}_2) \le 0 \\ \quad l(\boldsymbol{x}, \boldsymbol{y}_1, \boldsymbol{y}_2) = 0 \end{cases} \tag{38}$$

where $\boldsymbol{x}$ is the decision variable vector consisting of wind power capacity; additionally, $\boldsymbol{y}_1$ and $\boldsymbol{y}_2$ are, respectively, the day-ahead and intra-day decision variable vectors.

The scheduling problem of WPHSH systems is involved in the proposed capacity optimization problem, which is formulated as a mixed-integer linear model (MILP). A novel nested algorithm consisting of inner and outer models is constructed to solve the proposed multi-objective capacity optimization problem. The algorithm flow of the multi-objective optimization model presented in this paper is shown in Figure 4. Firstly, the pre-given wind power capacity is converted to the inner model. In the inner scheduling problem, the day-ahead and intra-day schedules of WPHSH systems under the given wind power capacity from the outer optimization model are optimized simultaneously, and the values of objectives 2 and 3 are obtained. The inner optimization model can be expressed as (39):

$$\begin{aligned} &\min\ f_{\mathrm{PVD}}(\boldsymbol{y}_1) + f_{\mathrm{POD}}(\boldsymbol{y}_1, \boldsymbol{y}_2) \\ &s.t.\ h(\boldsymbol{x}^*, \boldsymbol{y}_1, \boldsymbol{y}_2) \le 0 \\ &\quad\ l(\boldsymbol{x}^*, \boldsymbol{y}_1, \boldsymbol{y}_2) = 0 \end{aligned} \tag{39}$$

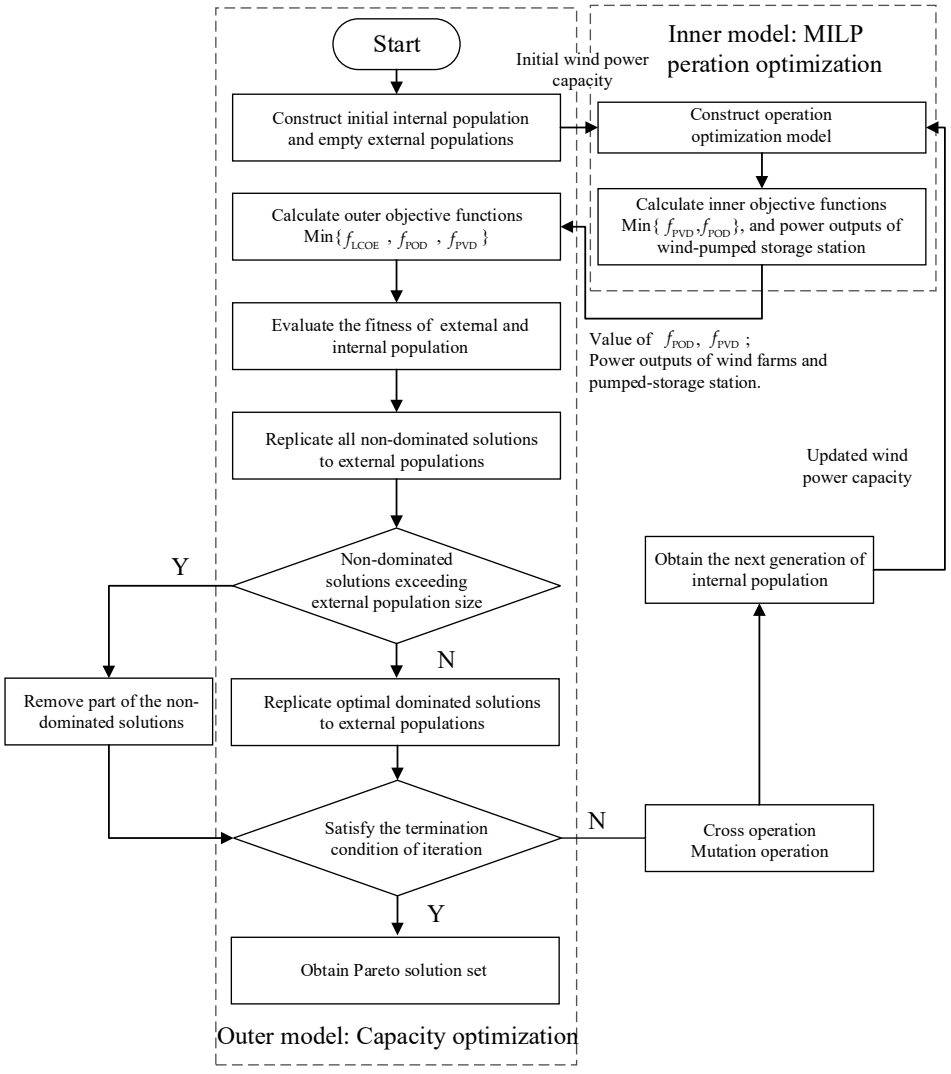

Figure 4. Flow chart of the optimization algorithm.

Subsequently, the values of objective functions 2 and 3 and the optimal schedule for the WPHSH systems is converted to the outer optimization problem. The outer optimization model utilizes strength Pareto evolutionary algorithm II [35,36] to calculate fitness functions

and generate the decision variable particles, which reflect the wind capacity. The updated wind power capacity is converted to inner optimization. With the iteration process, the Pareto optimal solution set can finally be obtained.

5. Case Study

5.1. Case Parameters

In this paper, based on the data for one year of wind power generation covering a region in northwest China, a combined GAN and K-means clustering algorithm is used to realize the aggregation of scenarios. The multilayer perceptron model is used for the generator and discriminator in the generative adversarial networks. The sigmoid function is selected as an activation function for the generator and discriminator. The learning rate is set to be 0.00001. Figure 5 shows the wind power output coefficient for ten typical days. The operational parameters are shown in Table 1, and the economic parameters are shown in Table 2.

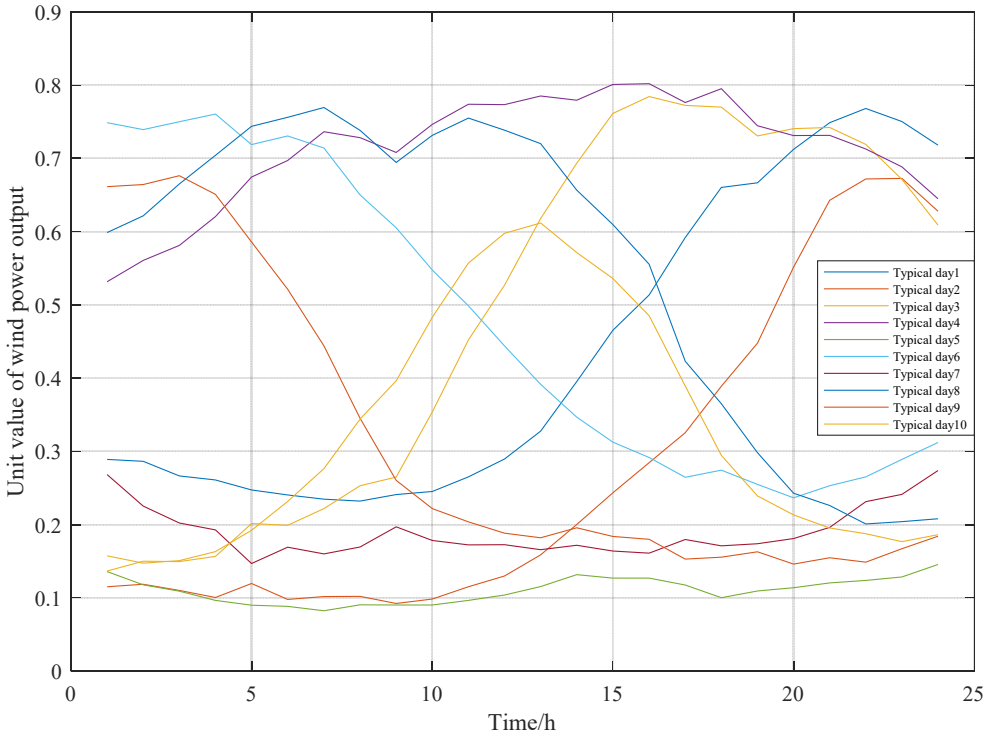

Figure 5. Per unit value curve of wind power output.

Table 1. System operational parameters.

Component	Operational Parameters	Value	Unit
Pumped storage	Upper reservoir	18,000,000	m^3
	Lower reservoir	18,000,000	m^3
	Water density	1000	kg/m^3
	Gravitational acceleration	9.81	m/s^2
	Pumped storage unit	300	MW
	Pipeline conveying efficiency	95%	--
	Pumping efficiency	80%	--
	Generating efficiency	90%	--
wind	Maximum installed capacity	2000	MW
	Discount rate	0.08	--
	Electricity purchase	0.075	USD/kwh

Table 2. The economic parameters.

Component	Economic Parameters	Value	Unit
Wind	Initial investment cost	1695	USD/kW
	Operation cost	51	USD/kW
	Degradation rate	0%	-
	Replacement cost	1695	USD/kW
	Expected lifetime	20	year
Fixed-speed pumped storage	Initial investment cost	453	USD/kW
	Operation cost	9.06	USD/kW
	Replacement cost	453	USD/kW
	Expected lifetime	15	year
Variable-speed pumped storage	Initial investment cost	985	USD/kW
	Operation cost	19.7	USD/kW
	Replacement cost	985	USD/kW
	Expected lifetime	15	year

5.2. Optimization Results

In the above sections, the capacity optimization model for wind–pumped hydro storage hybrid systems considering the uncertainty of wind power output was solved, and the Pareto solution set was analyzed. To show the trend of the Pareto frontier intuitively, the variation trends of each two objective functions are analyzed, as shown in Figures 6–8. Also, the installed wind power capacity and objective function values of points A, B, and C in Figures 6–8 are shown in Table 3.

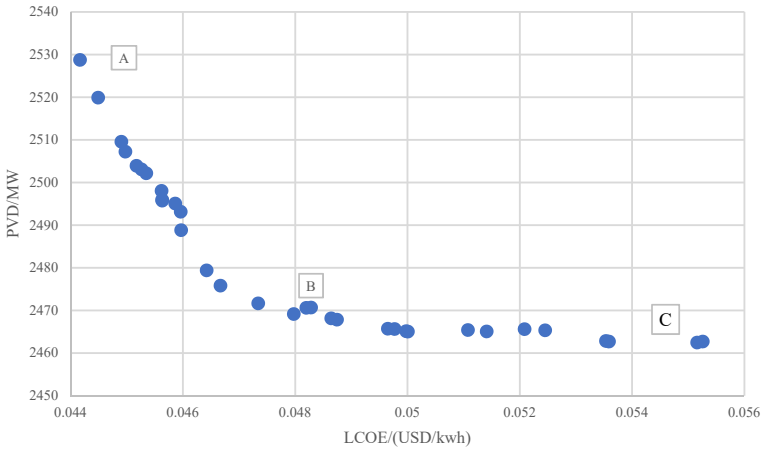

Figure 6. Relations between LCOE and PVD.

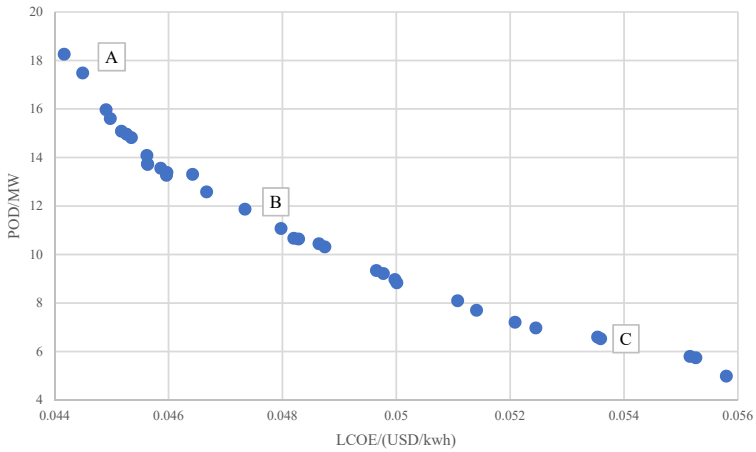

Figure 7. Relations between LCOE and POD.

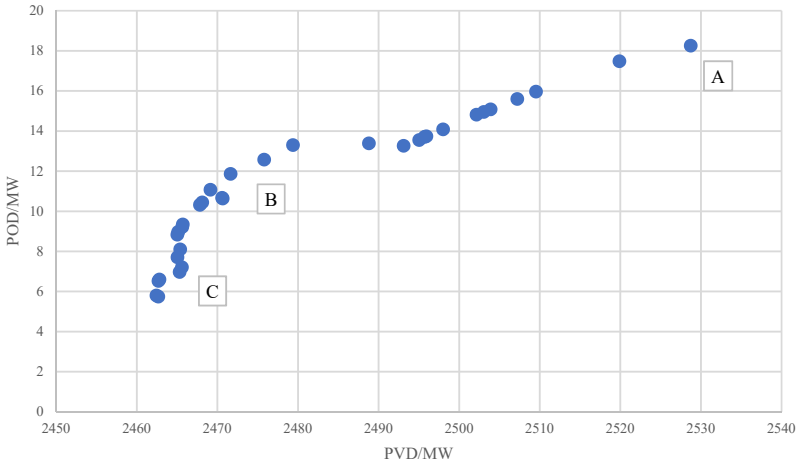

Figure 8. Relations between PVD and POD.

Table 3. Capacity of the wind turbine and optimization objective values.

	A	B	C
Installed capacity of wind turbine/MW	1429	956	532
LCOE/(USD/kwh)	0.044	0.047	0.053
PVD/MW	2528	2472	2462
POD/MW	18.2	11.8	6.5

Table 3 shows that from point A to point C, the total installed capacity of wind power decreases from 1429 MW to 532 MW, the LCOE increases from 0.044 USD/kWh to 0.047 USD/kWh, and the PVD decreases from 2528 MW to 2462 MW. Combined with Figure 6, it can be determined that as the installed capacity of wind power decreases, the output generation power of the hybrid system decreases, and the LCOE increases. At the same time, when the wind power installation capacity increases, the peak–valley difference of the net load of the regional power grid also increases due to the limitations of pumped storage regulation capabilities and reservoir capacity. Similarly, as seen in Figure 7, with a decrease in the installed capacity of wind power, the LCOE increases. Also, the wind power uncertainty caused by wind power was found to decrease, and the power outputs of WPHSH systems can be better stabilized, thus decreasing the POD of WPHSH systems. Figure 8 shows that increasing the installed capacity of wind power leads to a larger POD and PVD in WPHSH systems due to the anti-peak shaving characteristics and uncertainty of wind power.

5.3. Fixed-Speed and Variable-Speed Pumped Storage Operation Comparison Analysis

To illustrate the advantages of variable-speed pumped storage units in WPHSH systems, we set two cases as follows: Case 1: a pumped storage power station with three fixed-speed units and one variable-speed unit; Case 2: a pumped storage power station with four fixed-speed units.

The configuration scheme with a wind power capacity of 956 MW is selected in two cases, and the three objective functions of LCOE, PVD, and POD are compared and analyzed, as shown in Table 4. Table 4 shows that the economy of Case 2 is better with a lower LCOE, but the POD of Case 2 is larger since pumped storage with all the fixed-speed units cannot regulate power under pumping conditions. In addition, the operational flexibility of fixed-speed pumped storage units is worse than that of variable-speed units, leading to a larger PVD in Case 2.

Table 4. Comparison of the three objective function values.

	Case 1	Case 2
LCOE/(USD/kwh)	0.047	0.042
PVD/MW	2472	2547
POD/MW	11.8	21.9

The power outputs of pumped storage in the two cases are compared to demonstrate the advantages of variable-speed pumped storage in the hybrid system.

Figure 9 shows a comparison of the net load curve of Case 1 and Case 2 on a typical day 1. The water storage of the lower reservoir in the two cases is shown in Figure 10. As shown in Figures 9 and 10, from time intervals 3 to 8, the power loads are relatively low while wind power outputs are high, and the pumped storage units are operated under pumping conditions. In comparison, as fixed-speed pumped storage cannot adjust the power under pumping conditions, the pumped storage power station in Case 2 is continuously pumped with a fixed pumping power, resulting in the water storage of the lower reservoir approaching the minimum allowable storage limitation at time interval 7. Then, the pumped storage unit cannot maintain the pumping condition at time interval 8 to achieve load filling. Therefore, in Case 2, the valley of net loads appears at time interval 8. In contrast, in Case 1, the pumping power of the variable-speed pumped storage unit can be adjusted, and the pumping water flow can be changed accordingly. Therefore, the pumping condition can be maintained at time interval 8 so as to regulate the peak–valley of net loads better with the reservoir's operational constraints met.

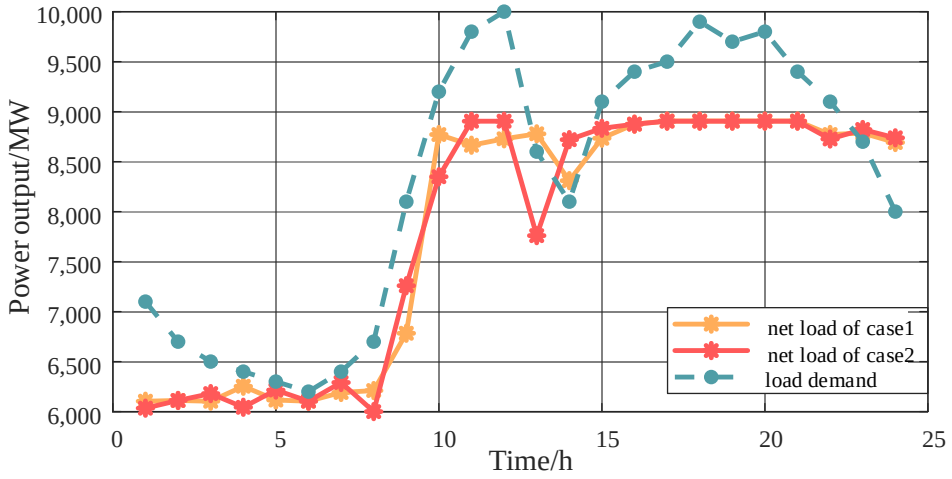

Figure 9. Load demand and net load curve of typical day 1.

At time intervals 3–8, the pumped storage power station operates under pumping conditions in Case 2. For the fixed-speed pumped storage unit, pumping power cannot be adjusted to compensate for the intra-day uncertainty of wind power outputs, leading to a larger POD. In contrast, the pumping power of the variable-speed pumped storage unit in Case 1 can be changed. As a result, when the pumped storage power station is under the pumping condition at time intervals 3–8, the intra-day power outputs of Case 1 are closer to the scheduled curve in the day ahead, leading to a lower POD.

To summarize, the pumped storage power station consisting of fixed- and variable-speed pumped storage units has a more ideal regulation effect and fluctuation stabilization ability, which is conducive to stabilizing the output deviation caused by the uncertainty of wind power output and promoting the facile grid connection of wind power.

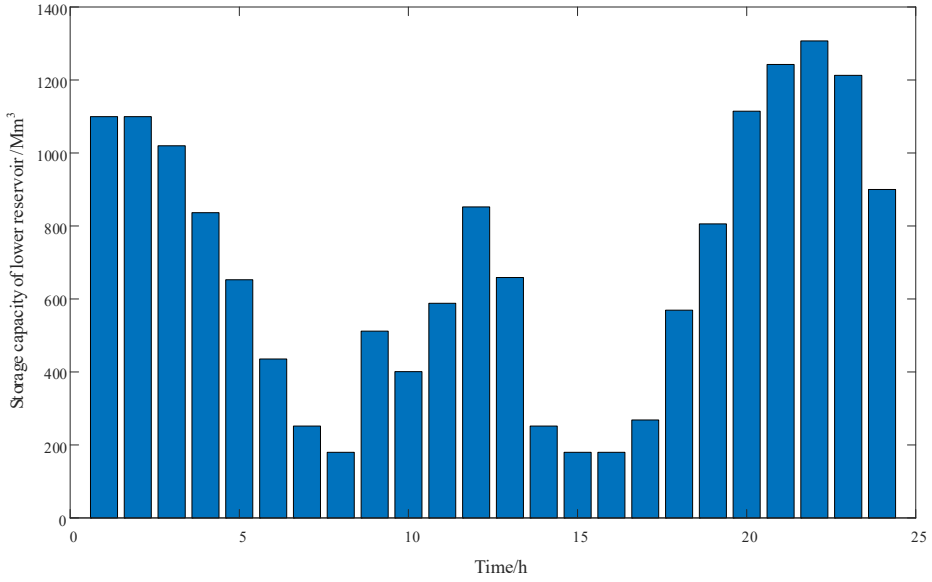

(**a**)

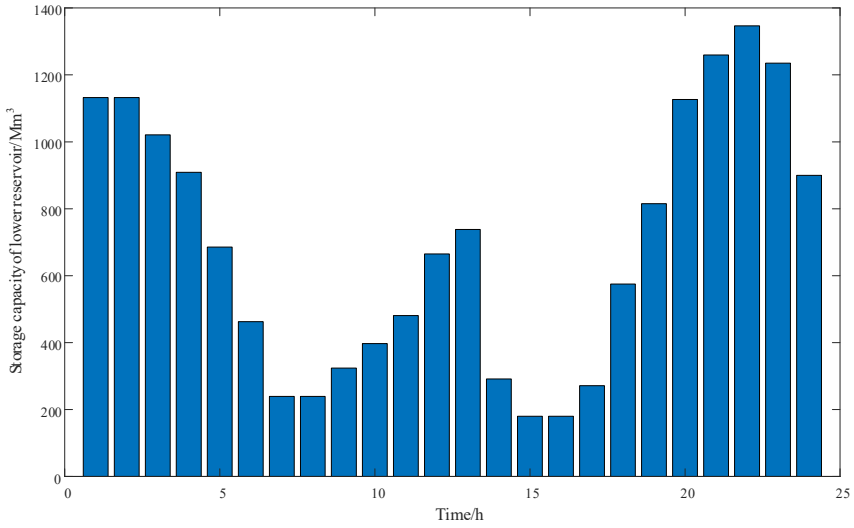

(**b**)

Figure 10. The real-time storage capacity of the lower reservoir on typical day 1. (**a**) The storage capacity of lower reservoir on typical day 1 of Case 1. (**b**) The storage capacity of the lower reservoir on typical day 1 of Case 2.

6. Conclusions

To improve the accommodation of wind power generation, we established a capacity optimization model for wind–pumped hydro storage hybrid systems considering variable-speed pumping characteristics. Three objectives were proposed: the levelized cost of energy, peak-shaving difference, and power output deviation. To formulate the fluctuation and uncertainty of wind power generation, the combined GAN and K-means clustering algorithm was presented to generate scenarios. In addition, an inner and outer iteration algorithm was proposed to solve the problem. Case studies show that with an increase in wind power installed capacity, the LCOE of the system decreases, the PVD increases, and the POD increases. Also, compared with fixed-speed pumped storage units, variable-speed pumped storage units have more ideal system-regulation and fluctuation-stabilization capabilities. With the increasing penetration of wind power connected to the power grid,

pumped storage power stations with a combination of fixed- and variable-speed units can not only meet the peak-shaving needs of the regional power grid but also reduce the impact of the uncertainty of wind power outputs on the power grid, which can ensure the safe and stable operation of the power grid.

Author Contributions: Conceptualization, Y.L. and O.L.; methodology, Y.L.; software, O.L.; validation, F.W. and S.M.; formal analysis, F.W.; investigation, S.M.; resources, L.S.; data curation, F.H.; writing—original draft preparation, O.L.; writing—review and editing, Y.L. and F.W.; visualization, S.M.; supervision, Y.L.; project administration, S.M. All authors have read and agreed to the published version of the manuscript.

Funding: This research was funded by the National Natural Science Foundation of China under grant number U23B20140 and 52107088l, the Natural Science Foundation of Jiangsu Province under grant number BK20210365, and the China Postdoctoral Science Foundation under grant number 2021M701039.

Data Availability Statement: Data are contained within the article.

Conflicts of Interest: Authors Shiyi Ma was employed by the company China Renewable Energy Engineering Institute. The remaining authors declare that the research was conducted in the absence of any commercial or financial relationships that could be construed as a potential conflict of interest.

References

1. Wang, Z.Z.; Wu, F.; Li, Y.; Li, J.Y.; Liu, Y.; Liu, W.E. Day-ahead dispatch approach for cascaded hydropower-photovoltaic complementary system based on two-stage robust optimization. *Energy* **2023**, *265*, 126145. [CrossRef]
2. Zhang, Y.Q.; Zhang, Z.; Zheng, J.H.; Zheng, Y.; Zhang, J.S.; Liu, Z.Q.; Fernandez-Rodriguez, E. Research of the array spacing effect on wake interaction of tidal stream turbines. *Ocean Eng.* **2023**, *276*, 114227. [CrossRef]
3. Guo, S.; He, Y.; Pei, H.J.; Wu, S.Y. The multi-objective capacity optimization of wind-photovoltaic-thermal energy storage hybrid power system with electric heater. *Sol. Energy* **2020**, *195*, 138–149. [CrossRef]
4. Wang, C.; Ju, P.; Lei, S.; Wang, Z.; Wu, F.; Hou, Y. Markov decision process-based resilience enhancement for distribution systems: An approximate dynamic programming approach. *IEEE Trans. Smart Grid* **2020**, *11*, 2498–2510. [CrossRef]
5. Wang, Z.Z.; Wu, F.; Li, Y.; Shi, L.J.; Lee, K.Y.; Wu, J.W. Itô-theory-based multi-time scale dispatch approach for cascade hydropower-photovoltaic complementary system. *Renew. Energy* **2023**, *202*, 127–142. [CrossRef]
6. Li, R.; Guo, S.; Yang, Y.; Liu, D.Y. Optimal sizing of wind/concentrated solar plant/ electric heater hybrid renewable energy system based on two-stage stochastic programming. *Energy* **2020**, *209*, 118472. [CrossRef]
7. Zhao, Z.; Zhang, M.; He, M.; Gao, Y.; Li, J.; Han, S.; Liu, Z.; Lei, L.; Díaz, J.I.P.; Cavazzini, G.; et al. Beyond fixed-speed pumped storage: A comprehensive evaluation of different flexible pumped storage technologies in energy systems. *J. Clean. Prod.* **2023**, 139994. [CrossRef]
8. Boroomandnia, A.; Rismanchi, B.; Wu, W.; Anderson, R. Optimal design of micro pumped-storage plants in the heart of a city. *Sustain. Cities Soc.* **2024**, *101*, 105054. [CrossRef]
9. Canales, F.A.; Jurasz, J.K.; Guezgouz, M.; Beluco, A. Cost-reliability analysis of hybrid pumped-battery storage for solar and wind energy integration in an island community. *Sustain. Energy Technol. Assess.* **2021**, *44*, 101062. [CrossRef]
10. Pradhan, A.; Marence, M.; Franca, M.J. The adoption of seawater pump storage hydropower systems increases the share of renewable energy production in small island developing states. *Renew. Energy* **2021**, *177*, 448–460. [CrossRef]
11. Pali, B.S.; Vadhera, S. An Innovative Continuous Power Generation System Comprising of Wind Energy Along With Pumped-Hydro Storage and Open Well. *IEEE Trans. Sustain. Energy* **2018**, *11*, 145–153. [CrossRef]
12. Perez-Diaz, J.I.; Jimenez, J. Contribution of a pumped-storage hydropower plant to reduce the scheduling costs of an isolated power system with high wind power penetration. *Energy* **2016**, *109*, 92–104. [CrossRef]
13. Bhayo, B.A.; Al-Kayiem, H.H.; Gilani, S.I.U.; Ismail, F.B. Power management optimization of hybrid solar photovoltaic-battery integrated with pumped-hydro-storage system for standalone electricity generation. *Energy Convers. Manag.* **2020**, *215*, 112942. [CrossRef]
14. Zohbi, G.A.; Hendrick, P.; Renier, C.; Bouillard, P. The contribution of wind-hydro pumped storage systems in meeting Lebanon's electricity demand. *Int. J. Hydrog. Energy* **2016**, *41*, 6996–7004. [CrossRef]
15. Yao, W.; Deng, C.; Li, D.; Chen, M.; Peng, P.; Zhang, H. Optimal Sizing of Seawater Pumped Storage Plant with Variable-Speed Units Considering Offshore Wind Power Accommodation. *Sustainability* **2019**, *11*, 1939. [CrossRef]
16. Ma, T.; Yang, H.X.; Lu, L.; Peng, J.Q. Optimal design of an autonomous solar-wind-pumped storage power supply system. *Appl. Energy* **2015**, *160*, 728–736. [CrossRef]
17. Gao, J.J.; Zheng, Y.; Li, J.M.; Zhu, X.M.; Kan, K. Optimal Model for Complementary Operation of a Photovoltaic-Wind-Pumped Storage System. *Math. Probl. Eng.* **2018**, *2018*, 5346253. [CrossRef]

18. Segurado, R.; Madeira, J.F.A.; Costa, M.; Duic, N.; Carvalho, M.G. Optimization of a wind powered desalination and pumped hydro storage system. *Appl. Energy* **2016**, *177*, 487–499. [CrossRef]
19. Xu, X.; Hu, W.H.; Cao, D.; Huang, Q.; Chen, C.; Chen, Z. Optimized sizing of a standalone PV-wind-hydropower station with pumped-storage installation hybrid energy system. *Renew. Energy* **2020**, *147*, 1418–1431. [CrossRef]
20. Yuan, W.; Xin, W.; Su, C.; Cheng, C.; Yan, D.; Wu, Z. Cross-regional integrated transmission of wind power and pumped-storage hydropower considering the peak shaving demands of multiple power grids. *Renew. Energy* **2022**, *190*, 1112–1126. [CrossRef]
21. Su, C.; Cheng, C.; Wang, P.; Shen, J.; Wu, X. Optimization model for long-distance integrated transmission of wind farms and pumped-storage hydropower plants. *Appl. Energy* **2019**, *242*, 285–293. [CrossRef]
22. Wang, R.; Yang, W.J.; Li, X.D.; Zhao, Z.G.; Zhang, S.S. Day-ahead multi-objective optimal operation of Wind-PV-Pumped Storage hybrid system considering carbon emissions. *Energy Rep.* **2022**, *8*, 1270–1279. [CrossRef]
23. Tang, Y.J.; Fang, G.H.; Tan, Q.F.; Wen, X.; Lei, X.H.; Ding, Z.Y. Optimizing the sizes of wind and photovoltaic power plants integrated into a hydropower station based on power output complementarity. *Energy Conv. Manag.* **2020**, *206*, 11. [CrossRef]
24. Zhu, Z.A.; Wang, X.; Jiang, C.W.; Wang, L.L.; Gong, K. Multi-objective optimal operation of pumped-hydro-solar hybrid system considering effective load carrying capability using improved NBI method. *Int. J. Electr. Power Energy Syst.* **2021**, *129*, 106902. [CrossRef]
25. Yang, W.J.; Yang, J.D. Advantage of variable-speed pumped storage plants for mitigating wind power variations: Integrated modelling and performance assessment. *Appl. Energy* **2019**, *237*, 720–732. [CrossRef]
26. Feng, C.; Zheng, Y.; Li, C.S.; Mai, Z.J.; Wu, W.; Chen, H.X. Cost advantage of adjustable-speed pumped storage unit for daily operation in distributed hybrid system. *Renew. Energy* **2021**, *176*, 1–10. [CrossRef]
27. Kumar, R.; Kumar, A. Optimal scheduling of variable speed pumped storage, solar and wind energy system. *Energy Sources Part A-Recovery Util. Environ. Eff.* **2021**. [CrossRef]
28. Chen, Y.Z.; Wang, Y.S.; Kirschen, D.; Zhang, B.S. Model-Free Renewable Scenario Generation Using Generative Adversarial Networks. *IEEE Trans. Power Syst.* **2018**, *33*, 3265–3275. [CrossRef]
29. Zhou, B.; Duan, H.R.; Wu, Q.W.; Wang, H.Z.; Or, S.W.; Chan, K.W.; Meng, Y.F. Short-term prediction of wind power and its ramp events based on semi-supervised generative adversarial network. *Int. J. Electr. Power Energy Syst.* **2021**, *125*, 106411. [CrossRef]
30. Li, S.; Ma, H.J.; Li, W.Y. Typical solar radiation year construction using k-means clustering and discrete-time Markov chain. *Appl. Energy* **2017**, *205*, 720–731. [CrossRef]
31. Benmouiza, K.; Cheknane, A. Forecasting hourly global solar radiation using hybrid k-means and nonlinear autoregressive neural network models. *Energy Conv. Manag.* **2013**, *75*, 561–569. [CrossRef]
32. Zhang, J.; Cheng, C.; Yu, S.; Su, H. Chance-constrained co-optimization for day-ahead generation and reserve scheduling of cascade hydropower–variable renewable energy hybrid systems. *Appl. Energy* **2022**, *324*, 119732. [CrossRef]
33. Wang, P.L.; Yuan, W.L.; Su, C.G.; Wu, Y.; Lu, L.; Yan, D.H.; Wu, Z.N. Short-term optimal scheduling of cascade hydropower plants shaving peak load for multiple power grids. *Renew. Energy* **2022**, *184*, 68–79. [CrossRef]
34. Liu, B.X.; Lund, J.R.; Liao, S.L.; Jin, X.Y.; Liu, L.J.; Cheng, C.T. Optimal power peak shaving using hydropower to complement wind and solar power uncertainty. *Energy Convers. Manag.* **2020**, *209*, 112628. [CrossRef]
35. Khaleghi, A.; Eydi, A. Multi-period hub location problem considering polynomial time-dependent demand. *Comput. Oper. Res.* **2023**, *159*, 106357. [CrossRef]
36. Pan, L.; Liu, X.; Jia, Z.; Xu, J.; Li, X. A multi-objective clustering evolutionary algorithm for multi-workflow computation offloading in mobile edge computing. *IEEE Trans. Cloud Comput.* **2023**, *11*, 1334–1351. [CrossRef]